35p.

SMITHSONIAN INSTITUTION
ASTROPHYSICAL OBSERVATORY

Research in Space Science

SPECIAL REPORT

Number 150

The Temperature Above the Thermopause

by

Luigi G. Jacchia

April 22, 1964

CAMBRIDGE, MASSACHUSETTS 02138

SAO Special Report No. 150

The Temperature Above the Thermopause

by

Luigi G. Jacchia

April 22, 1964

Smithsonian Institution
Astrophysical Observatory
Cambridge, Massachusetts 02138

THE TEMPERATURE ABOVE THE THERMOPAUSE[1]

by

Luigi G. Jacchia[2]

Summary--The conversion of upper-atmosphere densities to temperatures by means of atmospheric models, whether time-dependent or steady-state, is subject to limitations, which are critically examined. Nicolet's steady-state model is used to obtain temperatures from the drag of five artificial satellites in the time interval from 1958 to 1963. The temperature variations with solar and geomagnetic activity are reviewed. The relation between the day and night temperatures averaged over one solar rotation and the corresponding decimetric solar flux shows a definite departure from linearity, which is just about the same for the 8-cm and the 10.7-cm flux.

The diurnal variation is a very stable feature; its 2 PM maximum and 4 AM minimum do not show any appreciable shift with solar activity, nor does the ratio of the maximum to the minimum temperature, which is close to 1.30. An analytical model of the diurnal variation is presented as a function of solar time and latitude. This model is used to eliminate the day-and-night effect in a study of the semiannual temperature oscillation, whose amplitude is found to be related to solar activity in the same manner as the atmospheric temperature itself. The original explanation based on the solar wind now appears unlikely.

A practical method for the computation of exospheric temperatures as a function of geographic, solar, and geomagnetic parameters is schemetically presented.

Author

---

[1]This work was supported in part by grant No. NsG 87-60 from the National Aeronautics and Space Administration.

[2]Physicist, Smithsonian Astrophysical Observatory.

1. Densities and Temperatures

Nicolet (1960) showed that the increase of the density scale height with height, which is deduced from drag observations of artificial satellites, can be explained by assuming that above a certain height, called the thermopause, the temperature does not vary with height, while the mean molecular mass varies according to diffusion theory. At sunspot minimum, when the exospheric nighttime temperature is about 700° K, the thermopause is to be found at a height of about 220 km. For higher exospheric temperatures, the thermopause is correspondingly higher--300 km when the constant temperature is 1200° (average solar activity) and 400 km when the top temperature is 2000° (very high solar activity, daytime). Atmospheric-drag observations of satellites with perigees higher than 350 km yield entirely consistent temperatures at all heights when the densities are converted to temperatures with Nicolet's model (Jacchia, 1961; Jacchia and Slowey, 1963a). It therefore appears that Nicolet's model is a convenient tool for converting the atmospheric-density variations deduced from satellite drag into temperature variations, which can then be correlated with solar, geomagnetic, and geographic parameters. The temperatures derived in this manner refer to the region extending from the thermopause well into the exosphere. For simplicity we shall henceforth refer to them as exospheric temperatures.

All temperatures given in this paper were computed from densities deduced from satellite drag, using the latest version of Nicolet's model, extensive tabulations of which were kindly supplied to us by Dr. Nicolet. This new version differs from a previous one (Nicolet, 1961) in the treatment of He and H concentrations, which were taken according to later results by Kockarts and Nicolet (1962).

Densities were derived from atmospheric drag (i.e., from drag corrected for solar radiation-pressure effects) by applying Sterne's integral in its original form (Sterne, 1958) and using point-by-point numerical integration along the orbit, taking into account the rotation of the atmosphere. The density variation along the orbit was computed by first entering Nicolet's tables with a nighttime minimum temperature obtained from the 10.7-cm solar flux (Figure 1) and using the model of the diurnal variation described in Section 4; the process was then iterated with the temperature derived from the computed density.

The conversion of densities into temperatures by means of atmospheric models, and Nicolet's model in particular, is subject to some limitations, which it may be useful to enumerate:

1. The fact that satellites at different heights yield very nearly the same temperature at any given time, no matter how different this temperature may be from that observed at another time, gives assurance that the long-range temperature variations that are derived from the model are essentially correct. It does not prove, however, that the temperatures themselves are equally correct: they could all be systematically in error by a moderate amount owing to errors in the model's boundary conditions.

2. Since Nicolet's model is a steady-state model, it must be expected that systematic errors might affect even the temperature variations when the characteristic time of such variations is not much greater than the time of heat conduction from the lower thermosphere to the thermopause. This effect was clearly shown by Harris and Priester (1962a) in the case of the day-and-night variations. In their model, if we take a density at a given height when the temperature rises in the morning and read off the exospheric temperature at that instant, we find that the same density is reached with declining temperature in the evening when the exospheric temperature is considerably lower. In particular, the range of the diurnal variation may be systematically underestimated by using the steady-state model.

3. Even if we assume that Nicolet's model gives the correct relation between density and temperature at any given height during geomagnetically quiet days, we cannot be sure that this relation remains correct during geomagnetic disturbances, since the dissipation of energy that causes the heating during those disturbances cannot, except by a lucky accident, follow the same height distribution as the absorption of EUV, which is the main source of upper-atmospheric heating on quiet days. Fortunately the lucky accident seems close to being realized, inasmuch as the drag of low-perigee satellites shows that most of the heating during geomagnetic storms occurs at heights considerably lower than 200 km, in rough coincidence with the height of EUV absorption.

4. Variations of density ρ can be converted to variations of temperature T only when $\partial\rho/\partial T$ is large enough--which is generally the case for heights above 350 km. At 200 km the density is practically independent of temperature, making it impossible to derive temperatures from densities. The lower limit at which temperature determinations are still possible changes with the exospheric temperature, i.e., with solar activity. When the exospheric temperature approaches 2000°, it becomes hazardous to derive temperatures even at a height of 350 km (see Figure 3).

In the discussion that follows, all atmospheric temperatures have been derived from densities by means of Nicolet's model and must be understood to be subject to the aforesaid limitations.

The temperature variations observed above the thermopause are of four types:

1. Variations caused by changes in solar EUV radiation.

2. Variations correlated with geomagnetic activity.

3. The "diurnal" or "day-and-night" variation.

4. The semiannual variation.

Let us examine them one by one.

2. Temperature variations caused by changes in solar EUV radiation

As had been expected, the first continuous monitoring of solar EUV from the OSO-1 satellite (Neupert et al., 1963) showed a close parallelism between the intensity variations of individual spectral lines and the variations of the decimetric solar flux, which is commonly used as an EUV indicator in the study of upper-atmospheric variations (Priester and Martin, 1960; Jacchia, 1960). The OSO-1 observations covered an interval of a little over two months, from March to May, 1962, during which the 10.7-cm solar flux exhibited exceptionally strong and well-defined 27-day fluctuations, with maximum readings on the average 1.6 times larger than the minimum values. The corresponding intensity variations of λ 284 (Fe XV) and λ 335 (Fe XVI) were by a factor of 3 or 4, while those of the intense line λ 304 (He II) were much smaller, averaging only 25 percent. This great difference in behavior is due to the fact that the two iron emissions are confined mostly to the active plages on the sun, while the helium II line is emitted not only by the plages, but also from the quiet regions of the solar disk, as shown by recent rocket-borne NRL slitless spectrograms (Purcell et. al., 1963).

Since all EUV emissions contribute to the heating of the upper atmosphere, the relation between atmospheric temperature and EUV-line intensity must be different for each individual line, and the relation between exospheric temperature and any single monochromatic flux at decimetric wavelength cannot, obviously, be expected to be either simple or perfect. In particular, since the individual plage emissions are unlikely to keep their relative intensities unchanged in the course of a sunspot cycle, we must expect to find a different relation between EUV intensity and atmospheric heating, according to whether we determine it from variations within a time interval covering a 27-day solar rotation or from variations within an 11-year sunspot cycle. An analogous difference may be expected for similar reasons in the relation between the decimetric solar flux and atmospheric heating. This difference is actually observed (Jacchia, 1963), although its earlier interpretation, based on a solar-wind component in the 11-year cycle, is almost certainly wrong. Within a solar rotation the temperature was observed to vary by $2^{\circ}.5$ for every unit variation of the 10.7-cm solar flux, while the corresponding variation over a solar cycle is represented by a curve (Figure 1) with the average slope of $4^{\circ}.5$ at night and about $6^{\circ}.0$ in daytime. More recent observations seem to indicate that the temperature variation within a solar rotation has a value of $2^{\circ}.4$ near the daytime maximum and $1^{\circ}.9$ near the nighttime minimum, or just about 0.5 of the corresponding solar-cycle variation.

Nicolet (1963) claims that the relation between the temperature $\overline{T}$ and the decimetric flux $\overline{F}$, both averaged over one solar rotation, becomes linear when the 8-cm flux is used instead of the 10.7-cm flux. This is not confirmed by our observations. Nighttime minima and daytime maxima derived from the drag of five satellites with perigee heights between 350 and 658 km are given in Table 1, together with the corresponding values of the smoothed 10.7-cm and 8-cm solar fluxes. Table 2 gives results of the least-squares fitting, to the data of Table 1, of the

second-degree polynomial

$$\bar{T} = a + b(\bar{F} - 150) + c(\bar{F} - 150)^2 \ . \qquad (1)$$

As can be seen, the solutions for the 10.7-cm and for the 8-cm flux show no substantial difference in the values of the coefficient of the quadratic term. This could have been deduced from Nicolet's analysis itself, which shows that the relation between the two fluxes is linear in the interval between $\bar{F}_{10.7} = 70$ and $\bar{F}_{10.7} = 220$--i.e., over almost the whole range of Table 1--and starts departing from a linear relation only for $\bar{F}_{10.7} > 220$. Any significant curvature in the relation with the 10.7-cm flux should therefore also be present, with little change, in the relation with the 8-cm flux. Since the curvature is small anyhow, Nicolet's temperature calendar 1952-1962, computed using a linear relation between $\bar{F}_8$ and T, cannot be much in error.

3. Temperature variations correlated with geomagnetic activity

The correlation between geomagnetic index and upper-atmosphere temperature was shown to be practically linear on the basis of drag data from the Explorer IX satellite (Jacchia and Slowey, 1963b). Within the limitations described in Section 1 of the present paper, the temperature increase corresponding to a unit increase in the 3-hourly a_p index was found to be $1^\circ.0$ at low and moderate latitudes; when a correction is applied for the limited time resolution of the drag determinations, this value becomes $1^\circ.2$. The temperature variations appear to lag behind the geomagnetic variations by some five hours.

Injun III drag data (Jacchia and Slowey, 1964) show that the temperature increase is greater in the auroral zones by a factor as high as 3 or even 5 (Figure 5). Should the greater heating in the auroral zones prove to be connected with the occurrence of polar substorms, whose relation to the main phase is highly erratic (Akasofu and Chapman, 1963), we might expect the relation between temperature and a_p in the auroral zones to show a much greater scatter than at low latitudes.

No systematic temperature increase with latitude is indicated by the Injun III data on geomagnetically quiet days. An illustration of temperature variations with variable EUV and a_p is given in Figure 2.

4. The diurnal temperature variations

As can be seen from Figure 1, the daytime maximum temperatures are higher than the nighttime minima by a factor 1.30. Earlier determinations (Jacchia, 1961; Jacchia and Slowey, 1963a) had given for this factor values of 1.35 and 1.33. It is a remarkable feature of the diurnal variation that this factor seems to remain unchanged in the course of the

11-year sunspot cycle. This can be seen from Table 3, in which we give values of T_{max} and T_{min}, together with their ratios, computed from the independent quadratic least-squares solutions of Table 2.

Another stable feature of the diurnal variation is the hour of the maximum temperature, which occurs at 2 PM, with no discernible dependence on latitude or solar activity. The minimum of the temperature curve occurs around 4 AM and seems to be just a little flatter than the maximum.

By successive approximations, using the satellites of Table 1, whose orbital inclinations range from 33° to 50°, and the low-perigee satellites Injun III (inclination 70°) and Explorer XVII (inclination 58°), we have derived an analytical model of the temperature variations above the thermopause, which has been used to eliminate the diurnal variation in the analysis of the semiannual effect. Theoretical curves of the diurnal variation, computed with this model, are shown in Figures 3 and 4, for comparison with the observed data.

The model can be described as follows:

Let the temperature maximum occur at a point on the globe which has the same latitude as the subsolar point, and let the minimum nighttime temperature on the globe be T_0 and the maximum daytime temperature on the globe be RT_0. We shall assume that the daytime maxima T_D and nighttime minima T_N at any point on the globe are given by the equations

$$\begin{aligned} T_D &= T_0(1 + R \cos^m \eta) , \\ T_N &= T_0(1 + R \cos^m \theta) , \end{aligned} \tag{2}$$

where

$$\eta = 1/2(\varphi - \delta_\odot) ,$$

$$\theta = 1/2(\varphi + \delta_\odot) ,$$

where φ is the geographic latitude and $\delta_\odot$ the declination of the sun.

The temperature T at this given point can be expressed as a function of the hour angle H of the sun (the local solar time). Let us write

$$T = T_N(1 + A \cos^n \frac{\tau}{2}) , \tag{3}$$

with

$$A = \frac{T_D - T_N}{T_N} = R \frac{\cos^m \eta - \sin^m \theta}{1 + R \sin^m \theta} ,$$

and

$$\tau = H + \beta + p \sin(H + \gamma) \qquad (4)$$

$$(-\pi < \tau < \pi) ,$$

where β, γ and p are constants, and $H = 0$ corresponds to the sun's upper culmination.

The constant β determines the lag of the temperature maximum with respect to the sun's culmination, while p introduces in the temperature curve an asymmetry whose location is determined by γ. Replacing T_D and T_N from equation (1), we can write

$$T = T_0(1 + R \sin^m \theta)\left(1 + R \frac{\cos^m \eta - \sin^m \theta}{1 + R \sin^m \theta} \cos^n \frac{\tau}{2}\right) . \qquad (5)$$

Although in these equations the exponents m and n--which determine the mode of the longitudinal and the latitudinal temperature variations, respectively--are kept distinct, we find that in practice we can take $m = n$. An analysis of the aforementioned satellites yields the following set of constants:

$$R = 0.30$$

$$m = n = 2.5$$

$$\beta = -45^\circ$$

$$p = 12^\circ$$

$$\gamma = +45^\circ .$$

Isotherms on the globe computed from equation (4) using these constants are shown in Figure 6; the first of the maps represents the temperature distribution at the equinoxes; the second, that at the summer solstice. In both instances the minimum nighttime temperature was taken to be 1000° K. Curves of the temperature variation at the equinoxes for a point above the equator are shown, for low and for high solar activity, in Figure 7, together with the corresponding density variations at different heights. In these curves the nighttime minimum occurs at $3^h\ 47^m$ local solar time (counted from midnight), and the maximum at $14^h\ 13^m$.

Although R, m, n, β, p and γ were taken as constants, it is reasonable to assume that a more refined analysis with better data could show that a better solution may be obtained by making some of these parameters variable with height or latitude. The temperature curves obtained from different satellites, after correction for the diurnal variation according to this model, are in close inner agreement and do not show residuals in phase with the diurnal variation itself. We must conclude, therefore, that within the accuracy of the data the model with constant parameters appears to be quite satisfactory. In Figures 3 and 4 the diurnal variation, as computed from the above equations, is normalized to a constant amplitude.

5. The semiannual temperature variation

We can eliminate the diurnal effect from the temperatures T, derived from the drag of satellites with perigees variously located with respect to the sun, by reducing them to the nighttime minimum T_0 on the globe by means of the model of the diurnal variation described in Section 4. When the temperatures T_0 are all reduced to a standard value of the 10.7-cm solar flux by use of the relation shown on Figure 1, a semiannual oscillation becomes clearly apparent (Figure 8). Table 4 gives the mean values of $\overline{T}_0$ (smoothed to eliminate the variations due to the solar rotation) from 5 satellites and the corresponding values reduced to $\overline{F}_{10.7} = 175$; n is the number of satellites used at each date.

The semiannual variation was first detected by Paetzold and Zschörner (1960), who named it the "plasma effect" because they attributed its cause to the variable interaction between the solar wind and the atmosphere in the course of the earth's revolution around the sun. Paetzold and Zschörner (1961) also found an annual oscillation superimposed on the semiannual variation, and Paetzold (1962) speculated on the possibility of attributing its cause to the "interstellar wind," produced by the sun's motion relative to interstellar matter. Figure 9 shows the reality of this "annual" effect, whose result is to make the July minimum deeper than the January minimum and the October maximum higher than the April maximum.

The three other types of temperature variation, described in sections 2, 3 and 4, are all related to definite solar, geomagnetic, and geographic parameters. No such simple parameter can be found for the semiannual variation. The connection with the solar wind proposed by Paetzold was based mainly on the fact that the times of the maxima and minima closely coincide with those of the semiannual variation of geomagnetic activity (Bartels, 1932).

There are several objections to the plasma hypothesis, which can be summarized as follows:

1. The amplitude of the semiannual oscillation is proportional to the 10.7-cm flux (Figures 8, 9, 10) and therefore should also be closely proportional to the EUV flux. From space probes, from the diurnal geomagnetic variation in the polar regions, and from the tails of comets we can infer that no similar variation is likely to occur in the quiet component of the solar wind.

2. The semiannual variation in the geomagnetic index results from greater frequency of geomagnetic disturbances around the equinoxes. The annual K_p or A_p curve looks relatively smooth only because, to obtain it, means have to be taken over several years. No smooth systematic variation of the K_p index is observed within one year, while the semiannual temperature variation is quite smooth.

3. Since the relation between the geomagnetic index and the atmospheric temperature is known (see Section 3) and cannot by any means explain the semiannual variation, even if the semiannual variation of the geomagnetic index were smooth, it would be necessary to invoke another heating mechanism by the solar wind, entirely different from that which operates during geomagnetic disturbances, no matter how small.

4. To explain a semiannual variation in the interaction between the solar wind and the atmosphere, only two possibilities come to mind. The first is that the solar plasma flows out of the sun in thin streams from the spot regions, and that the earth in its yearly orbit, inclined to the sun's equator, crosses denser regions of the plasma twice a year. This hypothesis requires the streams to be unrealistically thin--of 9° to 18° half-width, according to Priester and Cattani (1962)--and the postulated relation with sunspots practically precludes the possibility of a smooth effect. The second hypothesis is based on the fact that the earth's dipole axis changes its position with respect to the sun, with the result that during the second half of the year the variation is the same as in the first half, except for the inversion of the poles. This is actually only the statement of a fact, but no suggestion on how this variation could possibly affect atmospheric heating has ever been advanced.

Johnson (1964) has recently suggested a convective mechanism that could explain the semiannual temperature variation. His idea is that during solstices the excess of heat input at the summer pole sets off convection currents at ionospheric levels with a meridional component directed from the summer pole toward the winter pole. The evected gas at the summer pole is replaced by gas from below, so that there is a rising motion; at the winter pole, on the other hand, there must be sinking of gas from the hotter regions above to the cooler and denser regions below the thermopause, with resulting heat transfer. The net result is a subtraction of heat from ionospheric levels whenever meridional flow exists, i.e., around solstices; around the equinoxes, when the two poles are equally heated, there is no meridional flow and the thermospheric and exospheric temperatures all over the globe are higher.

From an analysis of meteor-trail winds observed at Adelaide and at Jodrell Bank, Kochanski (1963) found an annual wind variation in the 70-to-100-km layer with a meridional component directed from the summer pole to the winter pole, just as required by Johnson's mechanism. Kochanski's meridional flows have maximum velocities of about 12 m/sec, in excellent agreement with the velocities required by Johnson (10 m/sec).

The one thing that is not evident from Johnson's mechanism is why the maxima and minima in the semiannual temperature variation should systematically differ from each other (Paetzold's "annual effect"). One can think of the eccentricity of the earth's orbit with the consequent variation of solar radiation in the course of the year, or of the systematic difference in the winter pole temperature at mesospheric levels. In any case, a marked difference between the meridional flow during the northern summer and that during the northern winter is apparent also in Kochanski's winds. The fact that the relative height of the maxima and minima in the temperature oscillation remains unchanged as the amplitude changes with the sunspot cycle (Figure 9) shows that the "annual" and the semiannual variations have the same origin.

Figure 9 shows that, although constantly present, the semiannual oscillation is a less stable feature than, say, the diurnal temperature variation; in particular, the times of maxima and minima can vary by well over one month. The significance of the lower temperatures in 1959 is not clear; they could be due to a temporary departure in the correlation between EUV and the 10.7-cm solar flux.

In connection with the 10.7-cm solar flux in the analysis of the semiannual effect, a misunderstanding by Nicolet (1963) should be cleared up. Nicolet suggests that the effect itself might be spurious and due to systematic instrumental errors in the measurement of the solar flux. In that case the semiannual effect should be present in the 10.7-cm flux--which is not true. Actually, the semiannual effect can easily be seen in the density plots from satellite drag before any correction for the solar flux (see Figure 3).

It must be pointed out that Johnson's lateral-heat transport mechanism should operate whenever there is a localized excess of heat input. In particular, it may have some effect in damping the amplitude of the diurnal variation, thus weakening one of the two reasons for invoking a second heat source (Harris and Priester, 1962a). As to the other reason--the late hour of the computed temperature maximum--Johnson thinks that it may prove possible to remove it, too, by the same process, although stronger winds would then become necessary. As was pointed out in Section 2, the maximum of the diurnal temperature variation remains remarkably constant at 2 PM throughout the solar cycle, whereas according to the two-source model it should shift from 3:30 PM at sunspot maximum to 11:45 AM at sunspot minimum, if the input angle of the second source is kept constant (Harris and Priester, 1962).

6. Summary of temperature variations

From the preceding sections we find that the procedure for computing the exospheric temperature T at any time is the following:

1. From $\bar{F}_{10.7}$, averaged over three solar rotations, derive the averaged nighttime minimum $\bar{T}_0$ using Figure 1 or equation (1).

2. Compute the nighttime minimum T_0' for the given day from the equation

$$T_0' = \bar{T}_0 + 1^\circ.9(F_{10.7} - \bar{F}_{10.7}) \ . \qquad (6)$$

3. Add a correction for the semiannual effect. An approximation to the variation shown in Figure 9 is given by the following equation:

$$T_0 = T_0' + \left(0^\circ.39 + 0^\circ.15 \sin 2\pi \frac{t - \text{Jun } 1}{365}\right) \bar{F}_{10.7} \sin 4\pi \frac{t - \text{Mar } 1}{365} \ . \qquad (7)$$

4. From T_0 compute T for the given hour and geographic location, using equation (5).

5. Add a correction for geomagnetic activity, according to Section 3.

Acknowledgement

The calculations involved in this paper were mostly performed on an IBM-7094 machine using programs prepared by Mr. Jack Slowey. A detailed analysis and tabulation of the results will be published shortly by Mr. Slowey and this writer.

References

AKASOFU, S.-I., and CHAPMAN, S.

1963. The development of the main phase of magnetic storms. Journ. Geophys. Res., vol. 68, p. 125.

BARTELS, J.

1932. Terrestrial-magnetic activity and its relation to solar phenomena. Terr. Magn. Atmos. Electric., vol. 37, p.1.

HARRIS, I., and PRIESTER, W.

1962a. Time-dependent structure of the upper atmosphere. Journ. Atmos. Sci., vol. 19, p. 286.

1962b. Theoretical models for the solar-cycle variation of the upper atmosphere. Journ. Geophys. Res., vol. 67, p. 4585.

JACCHIA, L. G.

1960. A variable atmospheric-density model from satellite accelerations. Journ. Geophys. Res., vol. 65, p. 2775.

1961. A working model for the upper atmosphere. Nature, vol. 192, p. 1147.

1963. Electromagnetic and corpuscular heating of the upper atmosphere. In Space Research III, Proc. Third Internat. Space Sci. Symp., Ed., W. Priester, North-Holland Publ. Co., Amsterdam, p. 3.

JACCHIA, L. G., and SLOWEY, J.

1963a. Accurate drag determinations for eight artificial satellites; atmospheric densities and temperatures. Smithsonian Contr. Astrophys., vol. 8, p. 1.

1963b. An analysis of the atmospheric drag of the Explorer IX satellite from precisely reduced photographic observations. Smithsonian Astrophys. Obs. Spec. Rep. No. 125, 57 pp.

1964. Atmospheric heating in the auroral zones: a preliminary analysis of the atmospheric drag of the Injun 3 satellite. Journ. Geophys. Res., vol. 69, p. 905.

JOHNSON, F. S.

1964. Circulation at ionospheric levels. Southwest Center for Advanced Studies, Report on Contract Cwb 10531, January 30.

KOCHANSKI, A.

1963. Circulation and temperatures at 70-to-100-kilometer height. Journ. Geophys. Res., vol. 68, p. 213.

KOCKARTS, G., and NICOLET, M.

1962. Le problème aéronomique de l'hélium et de l'hydrogène neutres. Ann. Géophys., vol. 18, p. 269.

NEUPERT, W. M., BEHRING, W. E., and LINDSAY, J. C.

1963. The solar spectrum from 50 angstroms to 400 angstroms. Goddard Space Flight Center, Rep. X-614-63-196.

NICOLET, M.

1960. Les variations de la densité et du transport de chaleur par conduction dans l'atmosphère supérieure. In Space Research I, Proc. First Internat. Space Sci. Symp., Ed., H. Kallmann-Bijl. North-Holland Publ. Co., Amsterdam, p. 46.

1961. Density of the heterosphere related to temperature. Smithsonian Astrophys. Obs. Spec. Rep. No. 75, 30 pp.

1963. Solar radio flux and temperature of the upper atmosphere. Journ. Geophys. Res., vol. 68, p. 6121.

PAETZOLD, H. K..

1962. Corpuscular heating of the upper atmosphere. Journ. Geophys. Res., vol. 67, p. 2741.

PAETZOLD, H. K., and ZSCHÖRNER, H.

1960. Bearings of Sputnik III and the variable acceleration of satellites. Space Research I. Proc. First Internat. Space Sci. Symp., Ed., H. Kallmann-Bijl, North-Holland Publ. Co., Amsterdam, p. 24.

1961. The structure of the upper atmosphere and its variations after satellite observations. Space Research II. Proc. Second. Internat. Space Sci. Symp., Ed., H. C. van de Hulst, C. de Jager, and A. F. Moore, North-Holland Publ. Co., Amsterdam, p. 958.

PRIESTER, W., and CATTANI, D.

1962. On the semiannual variation of geomagnetic activity and its relation to the solar corpuscular radiation. Journ. Atmos. Sci., vol. 19, p. 121.

PRIESTER, W., and MARTIN, H. A.

1960. Solare und tageszeitliche Effekte in der Hochatmosphäre aus Beobachtungen künstlicher Erdsatelliten. Mitt. Univ.-Sternw. Bonn, No. 29.

PURCELL, J. D., GARRETT, D. L., and TOUSEY, R.

1963. Spectroheliograms in the extreme ultraviolet. Paper presented at the 115th meeting of the Amer. Astron. Soc., Washington, D. C., Dec. 26-28. See also the report on this paper in Sky and Telescope, vol. 27, p. 213, April 1964.

STERNE, T. E.

1958. An atmospheric model, and some remarks on the inference of density from the orbit of a close earth satellite. Astron. Journ., vol. 63, p. 81.

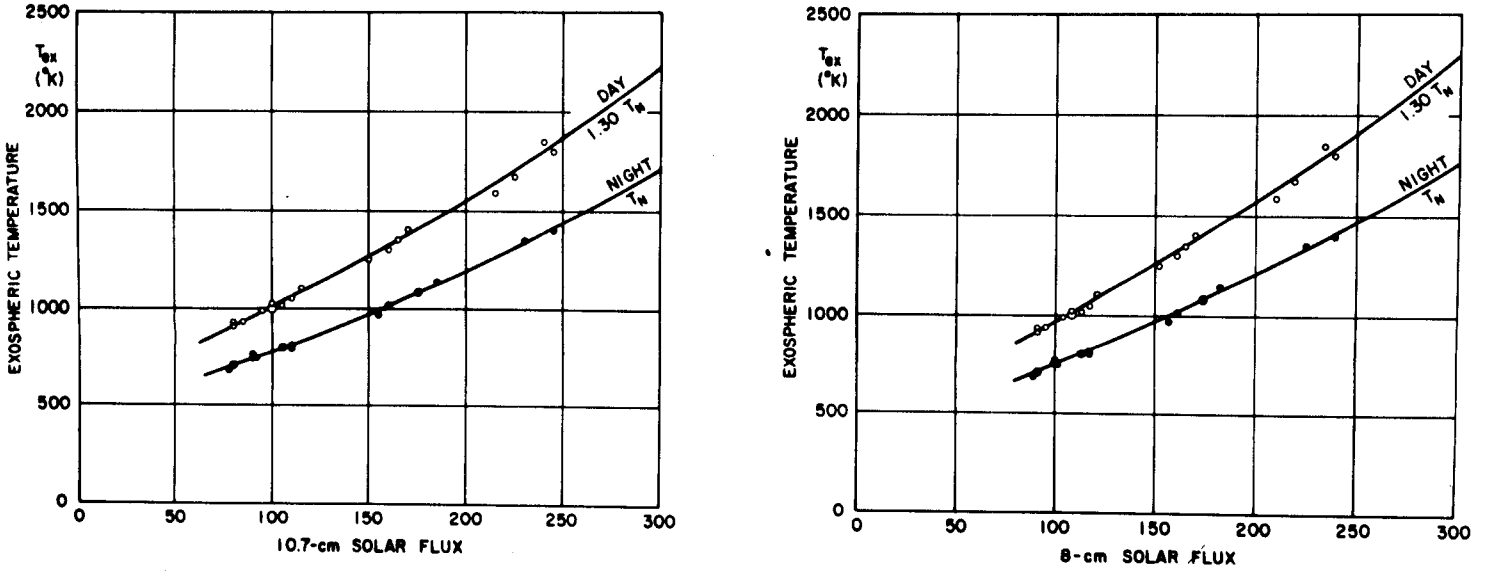

Figure 1.--Relation between day and night exospheric temperatures averaged over three solar rotations and the correspondingly smoothed solar flux at 10.7 and 8 cm (units of 10^{-22} watts/m^2/cycle /second bandwidth). The daytime-maximum curves were drawn through points corresponding to temperatures higher than the corresponding nighttime minima by a factor 1.30.

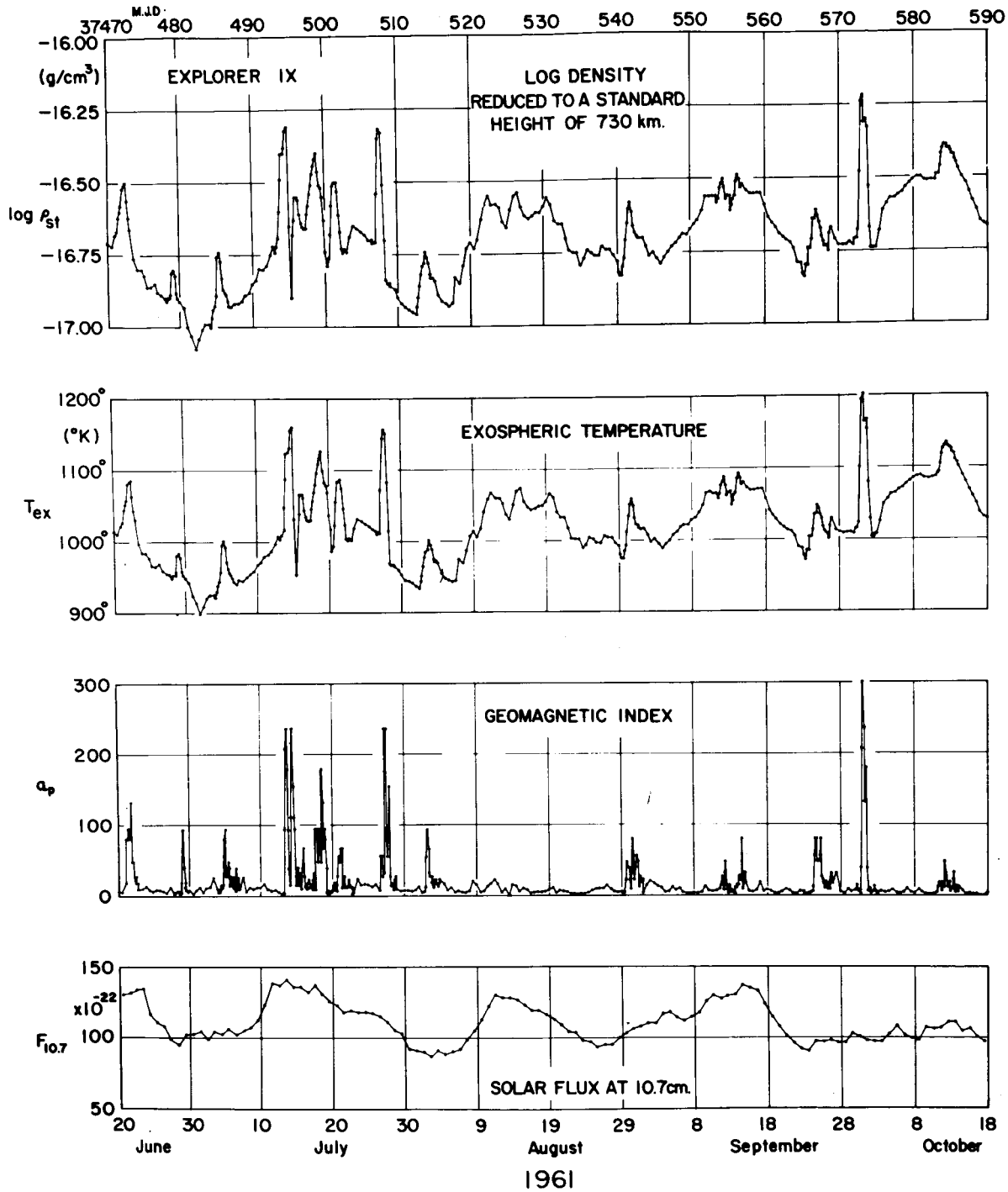

Figure 2.--Densities and temperatures derived from the drag of the Explorer IX satellite (1961 δ1), compared with the geomagnetic index a_p and the 10.7-cm solar flux. The drag was determined from precise position measurements on photographs taken with the Baker-Nunn cameras. MJD in the abscissa is the Modified Julian Day (JD minus 2 400 000.5).

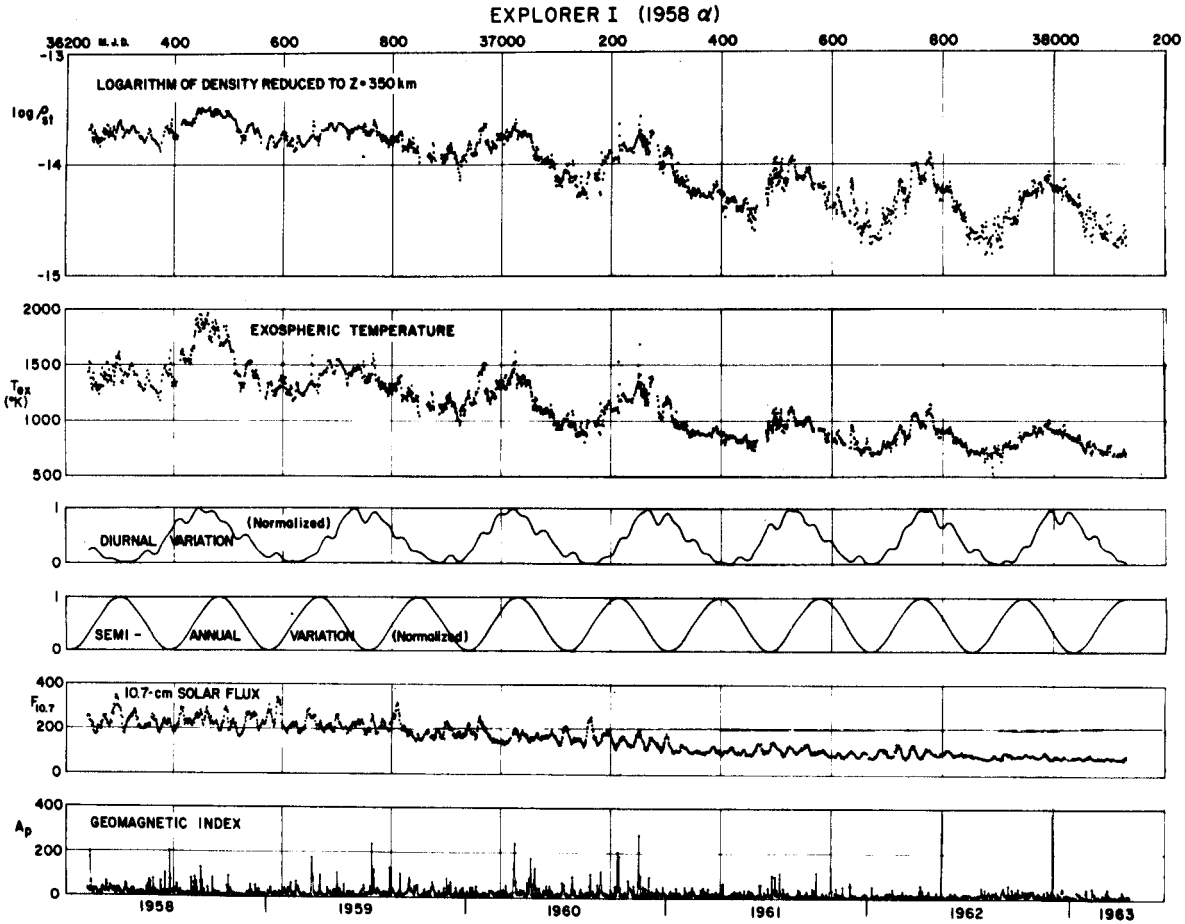

Figure 3.--Densities and temperatures derived from the drag of the Explorer I satellite (1958 Alpha), compared with solar and geomagnetic parameters. The diurnal-variation curve from equation (5), with constant amplitude, is shown for reference, as well as a constant-amplitude semiannual curve with maxima and minima roughly coincident with those of the temperature variation. The "wiggles" in the diurnal-variation curve are due to the rapid oscillations in latitude of the satellite's perigee; the perigee approaches the diurnal bulge from the morning side. Notice how the response in the density curve to temperature variations increases as the temperature decreases. MJD in the abscissa is the Modified Julian Day (JD minus 2 400 000.5).

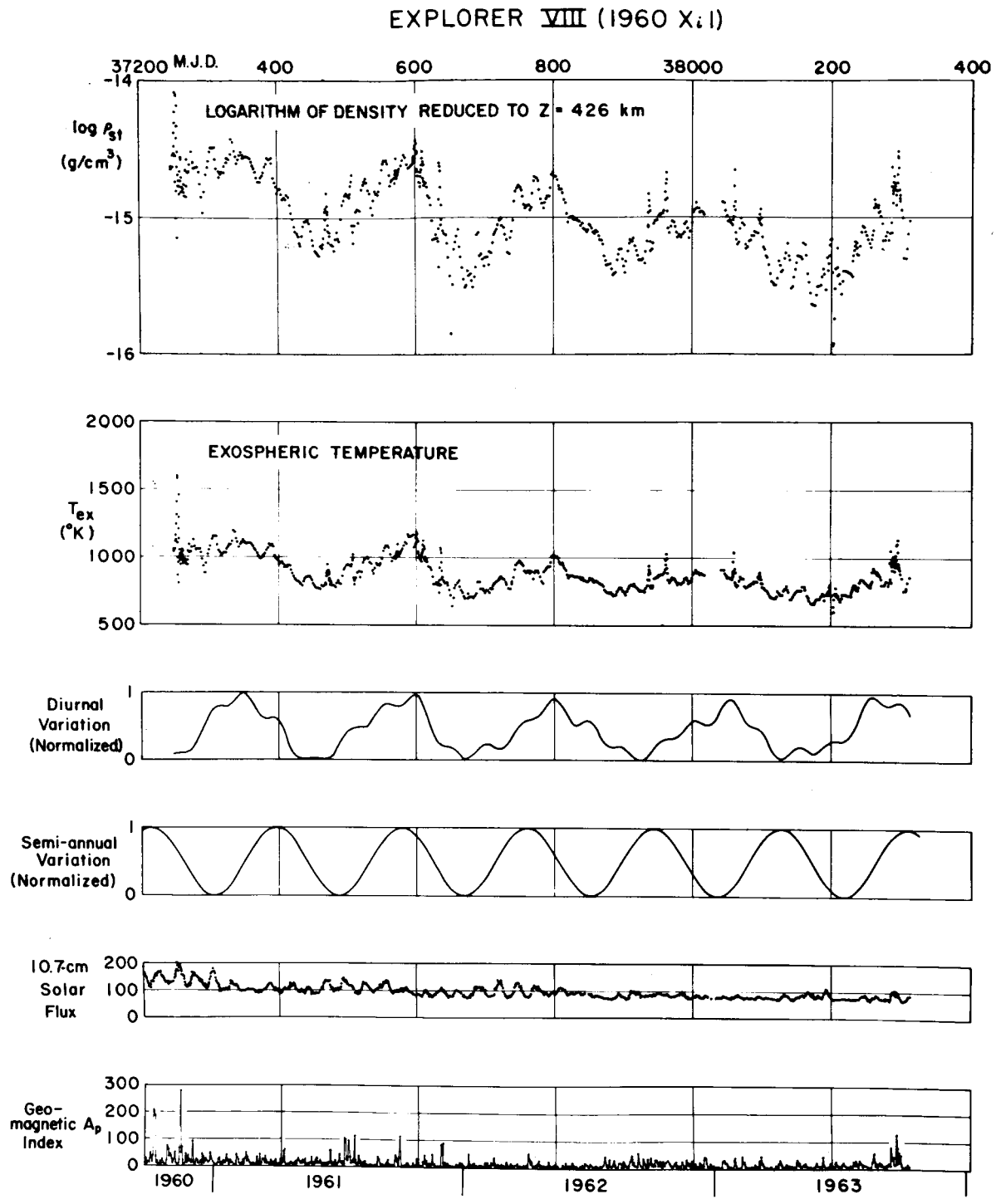

Figure 4.--Densities and temperatures derived from the drag of the Explorer VIII satellite (1960 ξ1), compared with solar and geomagnetic parameters. For fuller explanation see legend of Figure 3. The perigee of this satellite approaches the diurnal bulge from the evening side. MJD in the abscissa is the Modified Julian Day (JD minus 2 400 000.5).

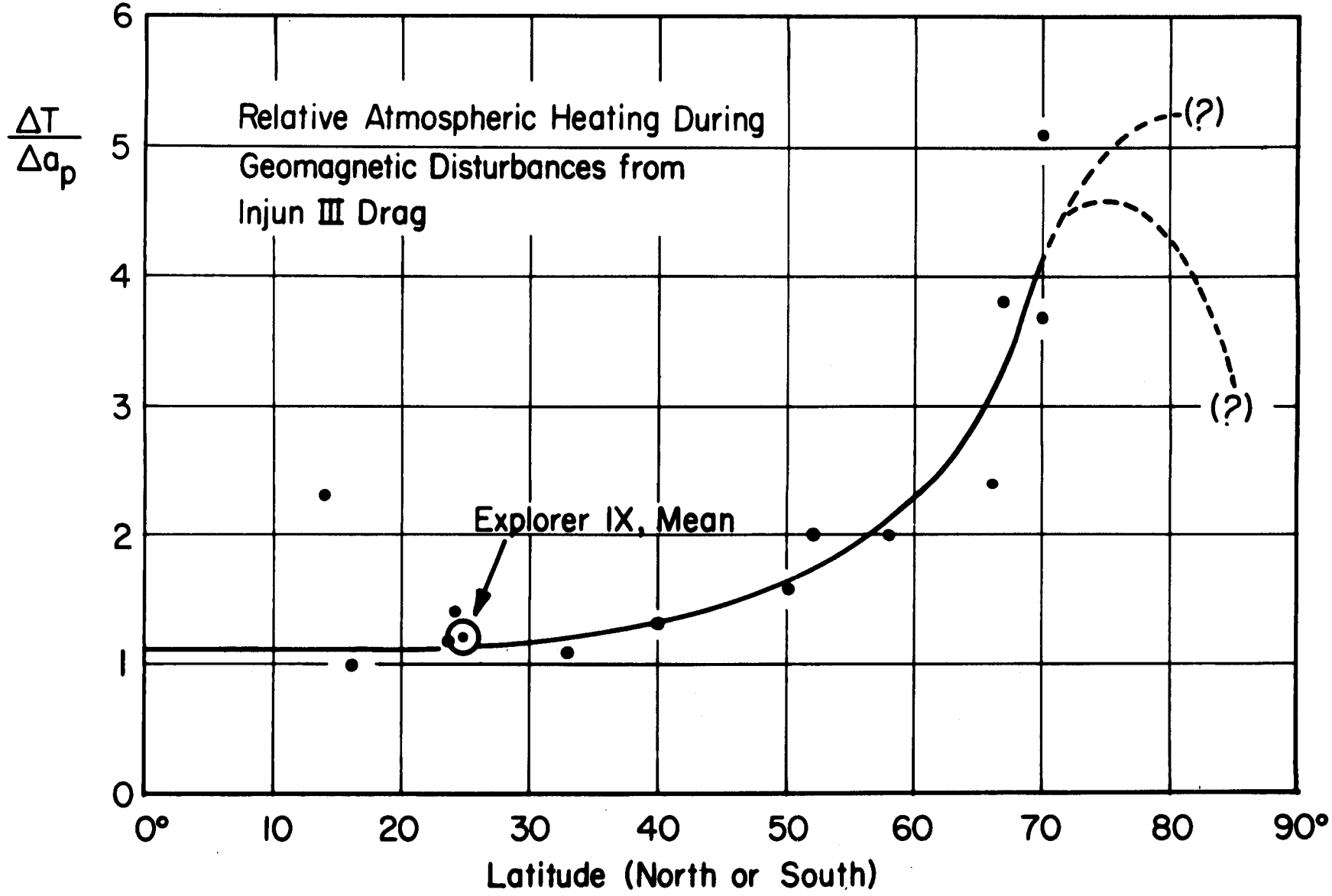

Figure 5.--Upper-atmospheric heating during geomagnetic storms as a function of geographic latitude. The limited time resolution involved in satellite drag determinations does not allow a meaningful distinction between geographic and geomagnetic latitude. Two speculative trends are indicated for latitudes higher than 70°.

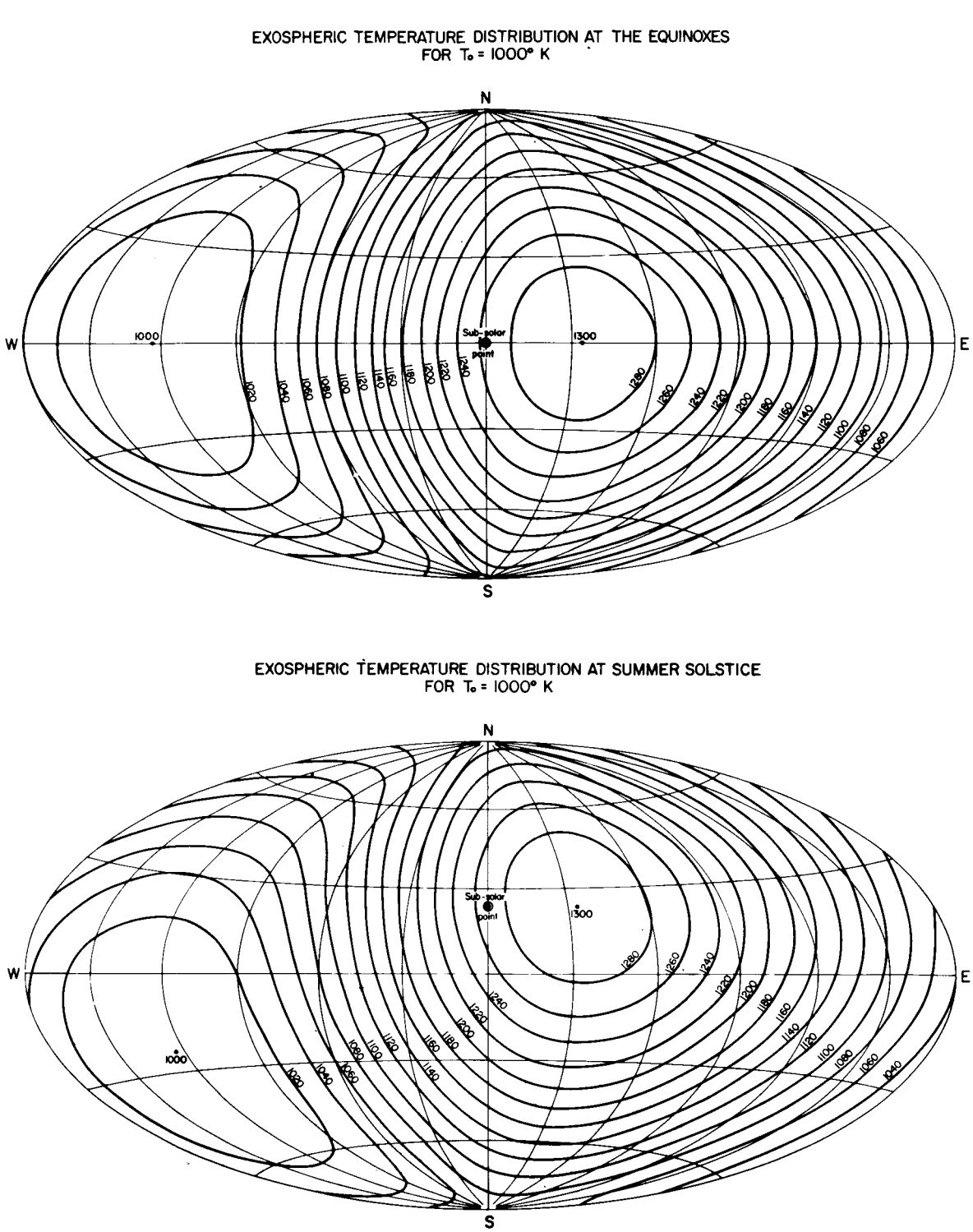

Figure 6.--Isotherms on the globe above the thermopause, computed from equation (5), taking T_o = 1000° K. Aitoff's equal-area projection; meridians and parallels are drawn 30° apart. Top, equinoxes; bottom, at summer solstice.

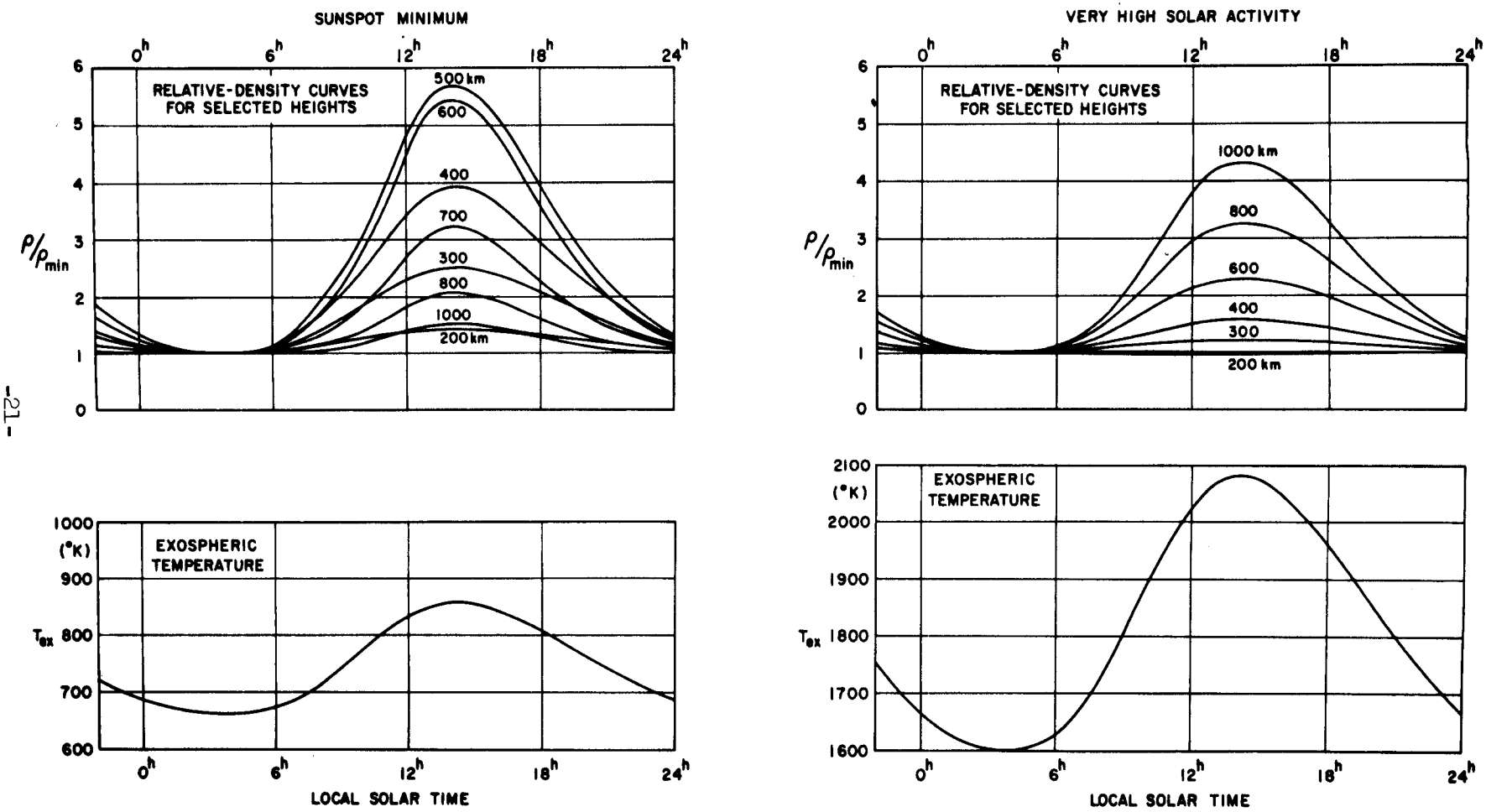

Figure 7.--Diurnal variation of the temperature above the thermopause, and of the density at different heights, at times of low and of very high solar activity. Densities from Nicolet's model.

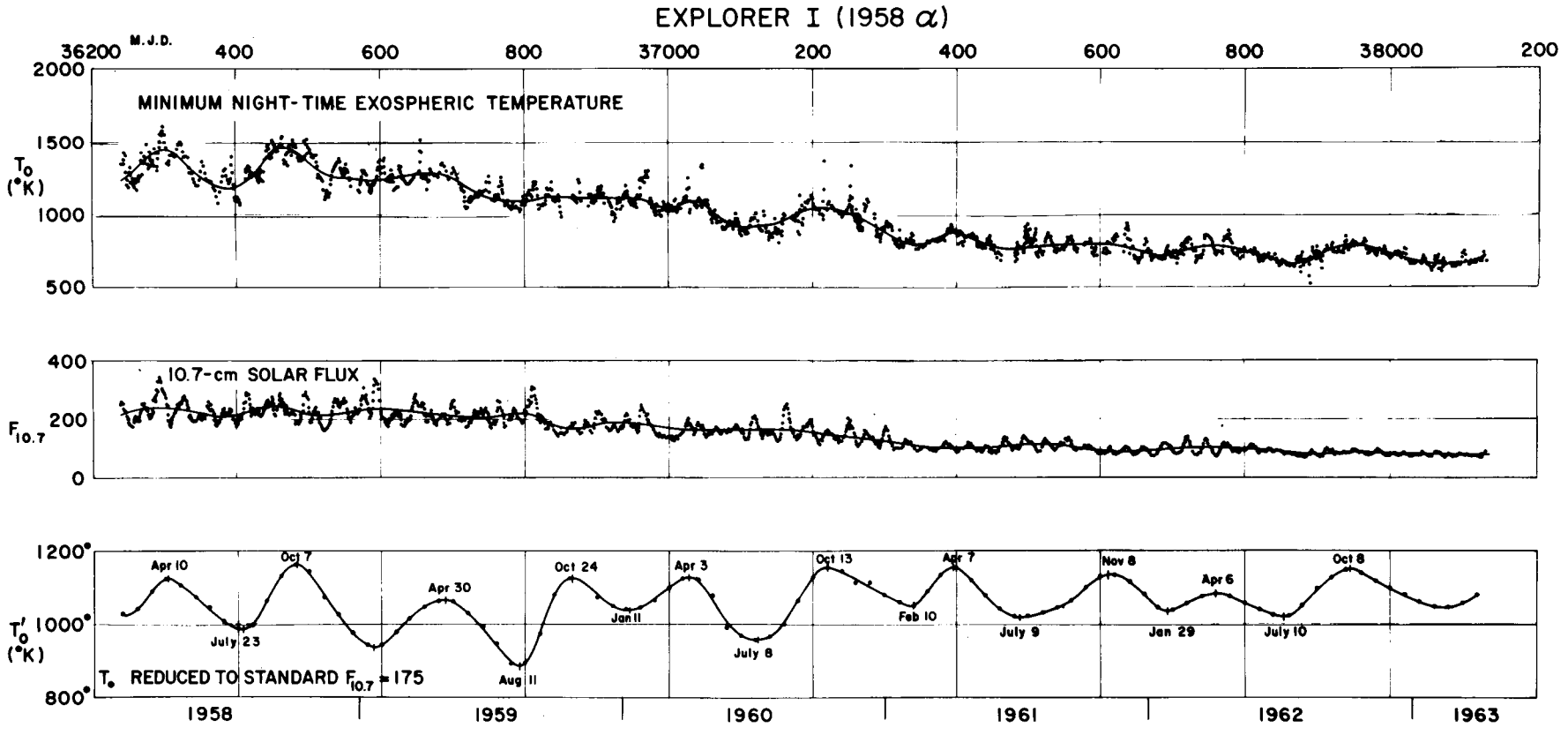

Figure 8.--The semi-annual effect derived from the drag of the Explorer I satellite (1958 Alpha). The minimum nighttime exospheric temperature T_o was computed using equation (5) from the temperatures (T_{ex}) of Figure 1. Smooth curves through T_o and $F_{10.7}$, the 10.7-cm solar flux, were used to eliminate the erratic ("27-day") fluctuations and the perturbations due to magnetic storms. When T_o is corrected to a standard solar flux using the relation of Figure 1, the bottom diagram is obtained.

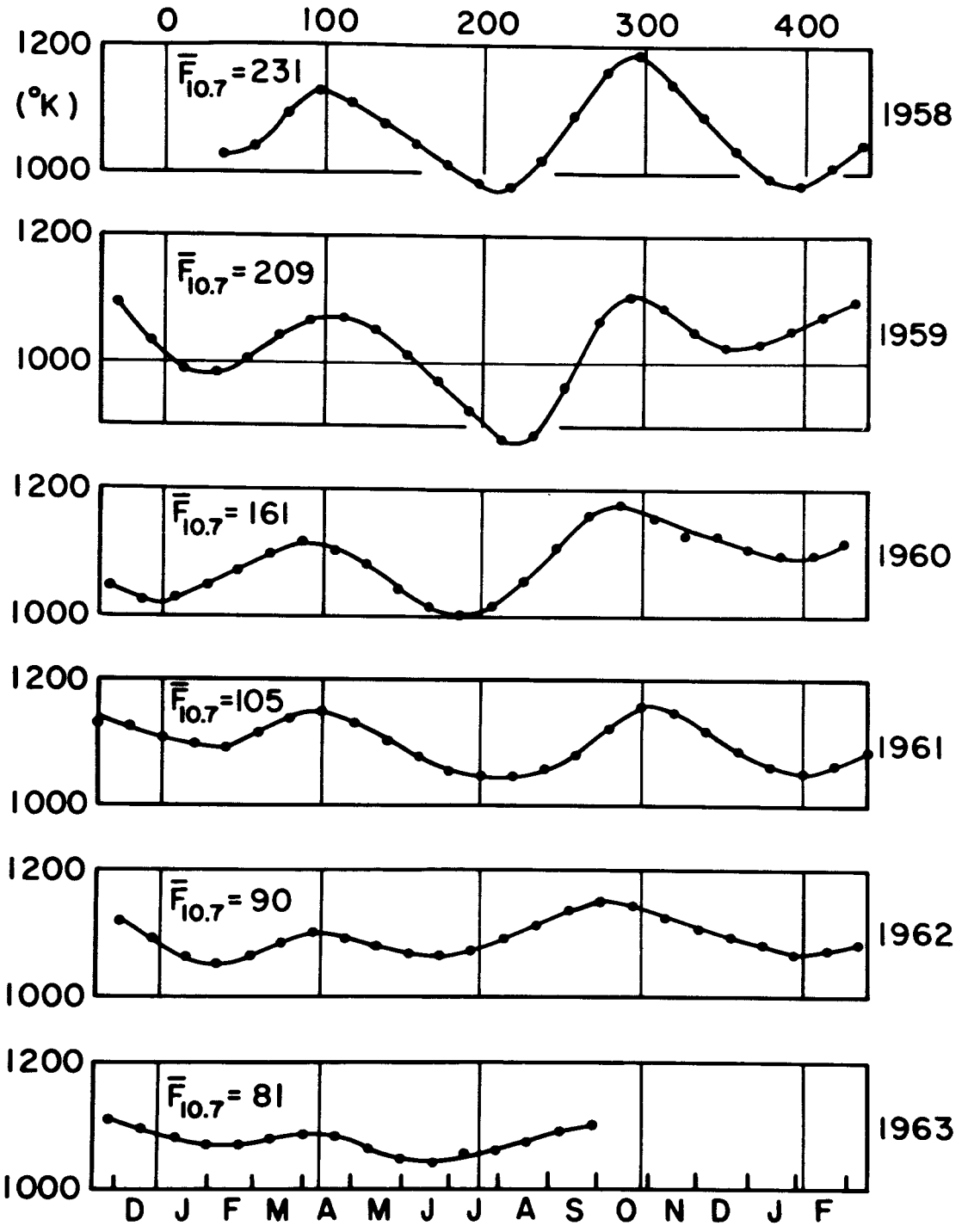

Figure 9.--The semiannual variation in the nighttime exospheric temperature from 1958 to 1963, as derived from the drag of five satellites. Days after January 1 at the top of the figure. Plotted are nighttime temperatures reduced to a standard 10.7-cm solar flux value of 175 (see Figure 7). The yearly average of $F_{10.7}$ is given for each year.

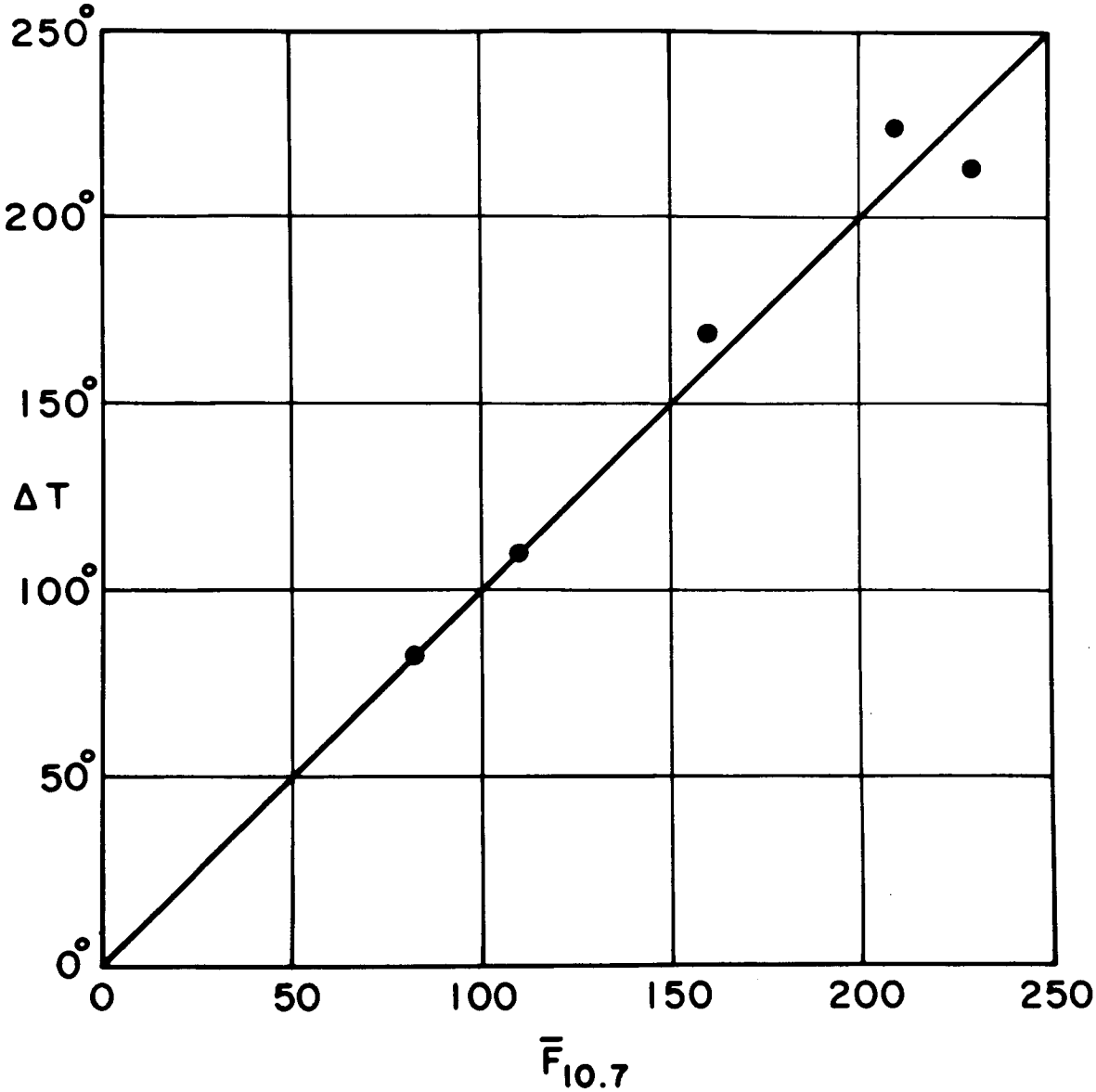

Figure 10.--The temperature difference between the July minimum and the October maximum of the semiannual variation in the nighttime exospheric temperature, plotted against the smoothed 10.7-cm solar flux.

Table 1.--Maxima and minima of the diurnal temperature variation from five satellites.

1. Nighttime minima

Year	$\bar{F}_{10.7}$	$\bar{F}_8$	$\bar{T}$	Satellite
1958.3	245	239	1400	1958 Alpha
1959.1	230	225	1350	1958 Alpha
1959.9	175	174	1080	1959 Eta
1959.9	185	182	1140	1958 Alpha
1960.0	175	174	1080	1959α1
1960.4	160	161	1020	1958β2
1960.6	155	157	975	1958 Alpha
1961.2	110	117	810	1959α1
1961.4	105	113	800	1958 Alpha
1961.4	105	113	800	1959 Eta
1961.5	110	117	800	1960ξ1
1962.0	92	101	740	1958 Alpha
1962.5	90	100	760	1959α1
1962.6	90	100	740	1960ξ1
1962.6	80	91	700	1958 Alpha
1963.2	80	91	700	1960ξ1
1963.3	78	89	680	1958 Alpha

Table 1.--Maxima and minima of the diurnal temperature variation from five satellites (continued)

2. Daytime maxima

Year	$\bar{F}_{10.7}$	$\bar{F}_8$	$\bar{T}$	Satellite
1958.7	245	239	1800	1958 Alpha
1958.9	240	234	1850	1958β2
1959.3	225	219	1675	1959α1
1959.5	215	210	1590	1958 Alpha
1960.3	165	165	1350	1958 Alpha
1960.6	160	161	1300	1959α1
1960.7	170	170	1400	1959 Eta
1960.9	150	152	1250	1958 Alpha
1961.1	115	121	1100	1960ξ1
1961.3	105	113	1020	1958β2
1961.6	110	117	1050	1958 Alpha
1961.8	100	108	1020	1959α1
1961.8	100	108	1010	1960ξ1
1962.2	100	108	1010	1959 Eta
1962.3	100	108	1010	1958 Alpha
1962.4	95	104	990	1960ξ1
1962.9	85	95	940	1958 Alpha
1963.0	80	91	930	1959α1
1963.0	80	91	920	1960ξ1

Table 2.--Least-squares fitting of the equation

$\bar{T} = a + b(\bar{F} - 150) + c(\bar{F} - 150)^2$ to the data of Table 1.

1. Nighttime minima

10.7-cm flux $\bar{F}_{10.7}$	8-cm flux $\bar{F}_8$
$a = 974^\circ.0 \pm 3^\circ.2$ (s.d.)	$a = 965^\circ.5 \pm 3^\circ.3$ (s.d.)
$b = 4^\circ.203 \pm 0^\circ.037$ (s.d.)	$b = 4^\circ.716 \pm 0^\circ.045$ (s.d.)
$c = 0^\circ.0042 \pm 0^\circ.0008$ (s.d.)	$c = 0^\circ.0034 \pm 0^\circ.0010$ (s.d.)

2. Daytime maxima

10.7-cm flux $\bar{F}_{10.7}$	8-cm flux $\bar{F}_8$
$a = 1258^\circ.1 \pm 6^\circ.4$ (s.d.)	$a = 1247^\circ.2 \pm 6^\circ.1$ (s.d.)
$b = 5^\circ.280 \pm 0^\circ.071$ (s.d.)	$b = 5^\circ.910 \pm 0^\circ.084$ (s.d.)
$c = 0^\circ.0070 \pm 0^\circ.0016$ (s.d.)	$c = 0^\circ.0069 \pm 0^\circ.0019$ (s.d.)

Table 3.--Maxima and minima of the diurnal temperature variation as a function of the smoothed 10.7-cm solar flux $\bar{F}_{10.7}$, from the least-squares fittings of Table 2.

$\bar{F}_{10.7}$	T_M	T_m	T_M/T_m
70	880°.8	664.7	1.325
120	1106.1	851.5	1.299
170	1366.5	1059.3	1.290
220	1662.2	1288.1	1.290
270	1993.0	1537.9	1.296

Adopted: T_M/T_m = constant = 1.30

Table 4.--Minimum nighttime temperatures

		$\bar{T}_o$	$\bar{F}_{10.7}$	$\bar{T}'_o$ ($\bar{F}_{10.7}$ = 175)	n
1958	Feb. 6	1225	218	1029	1
	Feb. 26	1300	231	1041	1
	Mar. 18	1395	240	1091	1
	Apr. 7	1440	242	1126	1
	Apr. 27	1387	235	1108	1
	May 17	1305	225	1074	1
	Jun. 6	1226	215	1044	2
	Jun. 26	1184	213	1012	2
	Jul. 16	1186	219	985	2
	Aug. 5	1241	232	977	2
	Aug. 25	1344	244	1020	2
	Sep. 14	1414	244	1090	2
	Oct. 4	1428	233	1159	2
	Oct. 24	1396	220	1190	2
	Nov. 13	1345	218	1149	2
	Dec. 3	1318	224	1093	2
	Dec. 23	1298	232	1034	2
1959	Jan. 12	1286	238	992	2
	Feb. 1	1287	240	983	2
	Feb. 21	1287	235	1008	2
	Mar. 13	1299	230	1045	3
	Apr. 2	1296	225	1065	3
	Apr. 22	1277	220	1071	3
	May 12	1227	213	1054	3
	Jun. 1	1163	208	1014	3
	Jun. 21	1118	207	974	3
	Jul. 11	1087	210	928	3
	Jul. 31	1076	218	880	3
	Aug. 20	1087	219	886	3
	Sep. 9	1097	205	962	3
	Sep. 29	1098	182	1067	3
	Oct. 19	1091	172	1104	4
	Nov. 8	1087	174	1092	4
	Nov. 28	1085	183	1050	4
	Dec. 18	1085	188	1028	4
1960	Jan. 7	1084	187	1031	4
	Jan. 27	1074	180	1052	4
	Feb. 16	1066	173	1074	4
	Mar. 7	1066	168	1097	4
	Mar. 27	1064	165	1120	4
	Apr. 16	1062	165	1105	4
	May 6	1033	164	1081	4
	May 26	992	163	1044	4
	Jun. 15	965	163	1017	4
	Jul. 5	958	164	1006	4
	Jul. 25	973	165	1016	4

Table 4.--Minimum nighttime temperatures (continued)

		$\bar{T}_o$	$\bar{F}_{10.7}$	$\bar{T}'_o$ ($\bar{F}_{10.7}$ = 175)	n
1960	Aug. 14	1008	164	1056	4
	Sep. 3	1050	161	1110	4
	Sep. 23	1072	153	1166	4
	Oct. 13	1066	148	1181	4
	Nov. 2	1036	146	1159	4
	Nov. 22	997	143	1132	5
	Dec. 12	948	131	1132	5
1961	Jan. 1	901	124	1112	5
	Jan. 21	861	116	1102	5
	Feb. 10	842	113	1096	5
	Mar. 2	837	106	1118	5
	Mar. 22	851	104	1140	5
	Apr. 11	858	103	1150	5
	May 1	845	104	1134	5
	May 21	827	106	1108	5
	Jun. 10	812	109	1081	5
	Jun. 30	807	114	1057	5
	Jul. 20	809	115	1055	5
	Aug. 9	807	115	1053	4
	Aug. 29	812	114	1062	4
	Sep. 18	818	110	1083	4
	Oct. 7	825	101	1125	4
	Oct. 28	826	92	1160	4
	Nov. 17	807	89	1152	4
	Dec. 7	778	89	1123	4
	Dec. 27	782	90	1093	4
1962	Jan. 16	767	94	1063	4
	Feb. 5	743	98	1054	4
	Feb. 25	767	101	1067	4
	Mar. 17	791	102	1087	4
	Apr. 6	799	100	1103	4
	Apr. 26	791	100	1095	4
	May 16	772	99	1080	4
	Jun. 5	747	95	1070	4
	Jun. 25	724	89	1069	4
	Jul. 15	713	85	1073	4
	Aug. 4	716	80	1096	4
	Aug. 24	736	80	1116	4
	Sep. 13	768	83	1136	3
	Oct. 3	793	85	1153	3
	Oct. 23	791	86	1148	3
	Nov. 12	766	85	1126	3
	Dec. 2	738	82	1110	3
	Dec. 22	714	79	1098	3

Table 4.--Minimum nighttime temperatures (continued)

		$\bar{T}_o$	$\bar{F}_{10.7}$	$\bar{T}_o'$ ($\bar{F}_{10.7}$ = 175)	n
1963	Jan. 11	695	78	1083	3
	Jan. 31	683	78	1071	3
	Feb. 20	684	78	1072	3
	Mar. 12	692	78	1080	3
	Apr. 1	707	80	1087	3
	Apr. 21	714	82	1086	2
	May 11	700	85	1061	2
	May 31	683	85	1044	2
	Jun. 20	664	81	1040	2
	Jul. 10	663	77	1055	2
	Jul. 30	668	77	1060	2
	Aug. 19	684	78	1072	2
	Sep. 8	712	80	1092	2
	Sep. 28	732	83	1100	2

Table 5.--Maxima and minima of the semi-annual temperature oscillation

	Min. I	Max. I	Min. II	Max. II	ΔT (Max. II - Min. II)	$\bar{F}_{10.7}$
1958		Apr. 10	Aug. 1	Oct. 20	215°	230
1958-1959	Jan. 23	Apr. 17	Aug. 9	Oct. 20	225°	210
1960	Dec. 26	Mar. 30	Jul. 9	Oct. 8	170°	160
1961	Feb. 1	Apr. 6	Aug. 1	Nov. 1	110°	110
1962	Feb. 4	Apr. 8	Jun. 27	Oct. 5	83°	82
1963	(Feb. 6)	Apr. 9	Jun. 20			
Mean	Jan. 21	Apr. 8	Jul. 17	Oct. 17		
Days after solstice or equinox	+30	+18	+26	+24		